



# Independent radiation of snailfishes into the hadal zone confirmed by *Paraliparis selti* sp. nov. (Perciformes: Liparidae) from the Atacama Trench, SE Pacific

Thomas D. Linley<sup>1</sup> · Mackenzie E. Gerringer<sup>2</sup> · Heather Ritchie<sup>3</sup> · Johanna N. J. Weston<sup>1</sup> · Amy Scott-Murray<sup>4</sup> · Vincent Fernandez<sup>4</sup> · Jhoann Canto-Hernández<sup>5</sup> · Frank Wenzhöfer<sup>6,7,8</sup> · Ronnie N. Glud<sup>6,9,10</sup> · Alan J. Jamieson<sup>11</sup>

Received: 28 January 2022 / Revised: 2 July 2022 / Accepted: 29 July 2022 / Published online: 1 October 2022  
© The Author(s) 2022

## Abstract

Snailfishes are among the most rapidly radiating families of marine fishes, resulting in a global distribution from the coastal intertidal to deep subduction trenches. The true diversity and distribution of deep-water snailfishes, particularly at hadal depths (>6000 m) and in the Southern Hemisphere, remain uncertain due to the rarity of samples. Here, we present the snailfish diversity at near-hadal and hadal depths in the Atacama Trench, which runs along the southwest coast of South America. Using free-fall baited cameras and traps, we documented at least three species of hadal snailfishes between 5920 and 7608 m based on distinct morphologies. One snailfish specimen was recovered from 6714 m, which we describe herein as *Paraliparis selti* sp. nov., based on a combined morphological and molecular taxonomic approach (16S, COI, and Cyt-b). *Paraliparis selti* sp. nov. is morphologically distinct from described snailfishes due to a combination of high number of; vertebrae (65) particularly the abdominal vertebrae (12), dorsal fin rays (60), anal fin rays (52), and caudal fin rays (8); comparatively low number of pectoral fin rays (18) which forms a deep notch with two widely spaced non-rudimentary rays. Micro-CT was used to minimise dissection of the specimen and to provide a digital holotype. *Paraliparis selti* sp. nov. highlights the importance of the Liparidae at hadal depths and provides evidence for at least two independent radiations of snailfishes into the hadal zone.

**Keywords** Liparidae · Phylogenetics · *Paraliparis* · Hadal · Perú–Chile Trench · South America · Micro-CT · DNA barcoding · Digital holotype

---

This article is registered in Zoobank under: <https://zoobank.org/5EE18E79-3035-45BA-9F60-E01C4C49CFB3>.

---

Communicated by R. Thiel

---

✉ Thomas D. Linley  
Thomas.Linley@newcastle.ac.uk

<sup>1</sup> School of Natural and Environmental Sciences, Newcastle University, Ridley Building, Newcastle-upon-Tyne NE17RU, UK

<sup>2</sup> State University of New York at Geneseo, Geneseo, NY 14454, USA

<sup>3</sup> Japan Agency for Marine–Earth Science and Technology (JAMSTEC), 2-15 Natsushima, Yokosuka, Kanagawa 237-0061, Japan

<sup>4</sup> Imaging and Analysis Centre, The Natural History Museum, Cromwell Road, London SW7 5BD, UK

<sup>5</sup> Jefe de Área Zoología Vertebrados, Museo Nacional de Historia Natural, Santiago, Chile

<sup>6</sup> Nordcee and HADAL, Department of Biology, University of Southern Denmark, 5230 Odense M, Denmark

<sup>7</sup> HGF-MPG Group for Deep Sea Ecology and Technology, Alfred Wegener Institute Helmholtz Center for Polar and Marine Research, 27570 Bremerhaven, Germany

<sup>8</sup> HGF-MPG Group for Deep Sea Ecology and Technology, Max Planck Institute for Marine Microbiology, 28357 Bremen, Germany

<sup>9</sup> Department of Ocean and Environmental Sciences, Tokyo University of Marine Science and Technology, Tokyo 108-8477, Japan

<sup>10</sup> Danish Institute of Advanced Study, University of Southern Denmark, 5230 Odense M, Denmark

<sup>11</sup> Minderoo-UWA Deep-Sea Research Centre, School of Biological Sciences and Oceans Institute, The University of Western Australia, IOMRC Building M470, 35 Stirling Highway, Perth, WA 6009, Australia

## Introduction

Snailfishes (Family Liparidae Gill, 1861) are a diverse teleost group. Over 400 species of snailfishes are found in every ocean. Closely followed by the Ophidiidae (Gerringer et al. 2021), the Liparidae hold the widest known bathymetric range of any vertebrate family, from the intertidal to the deep subduction trenches (Chernova et al. 2004; Fricke et al. 2020). At least 200 snailfish species are present in the Southern Hemisphere (Stein and Chernova 2002; Stein 2012), and of those, about 150 species are known from the Subantarctic and Antarctic waters (Chernova et al. 2004; Chernova and Prut'ko 2011; Stein 2012). Only six genera (~20 species) are known from the eastern Pacific off the west coast of South America (Stein 2005). These species represent a distinct Chilean group of liparids (Stein et al. 2001) including the endemic, monotypic genus, *Eknomoliparis* (Stein et al. 1991).

Despite the challenges to sample depths deeper than 6000 m, snailfishes are well-documented at hadal depths (Linley et al. 2016). Between 6000 to 8143 m, snailfishes dominate the hadal ichthyofauna in at least ten trenches worldwide (Jamieson et al. 2021). Snailfishes are exceptionally well-adapted to the hadal environment, which is characterised by low temperature (1–3°C), extremely high pressure, and seismic activity (Jamieson et al. 2010; Gerringer 2019). Currently, all described hadal snailfishes are ascribed to two genera (Linley et al. 2016; Gerringer 2019; Jamieson et al. 2021). In the Southern Hemisphere, *Notoliparis* Andriashev, 1975 contains *N. kermadecensis* Nielsen, 1964 and *N. stewarti* Stein, 2016 from the Kermadec Trench and *N. antonbruuni* Stein, 2005 from the Atacama Trench, the latter described from a single badly damaged specimen captured at 6150 m depth. *Pseudoliparis* Andriashev, 1955 is known from Northern Hemisphere and contains *P. belyaevi* Andriashev and Stein, 1998 and *P. amblystomopsis* Andriashev and Stein, 1998 from the Japan Trench, and *P. swirei* Gerringer and Linley, 2017 from the Mariana and Yap Trenches. In addition to these truly hadal species, near-hadal snailfishes are also known from the genus *Careproctus* Krøyer, 1862, specifically *Careproctus sandwichensis* Andriashev and Stein, 1998 from 5435 to 5453 m in the South Sandwich Trench, Southern Ocean. Further, at least six hadal liparid species have been observed on camera but lack voucher specimens needed for description (see Jamieson et al. 2021).

Although the importance of snailfishes at hadal depth is well-established, the true diversity and distribution of deep-water snailfishes remains uncertain due to comparatively lower sampling intensity and infrequent observations, coupled with new species being often described from single specimens in poor physical condition (Duhamel et al. 2010; Stein 2012). The visual identification of hadal snailfishes is particularly challenging, due to the frailty of the animals, the importance of internal characters such as vertebral counts and tooth

morphology in identifying species, and the difference between in situ and surface environmental conditions. For example, when a hadal specimen is recovered at the surface, their gelatinous layer, or subdermal extracellular matrix, begins to quickly deteriorate, changing the body proportions of the animal considerably (Gerringer et al. 2017a). The limited number of specimens, coupled with physical changes from recovery and preservation, result in a very different appearance between in situ imaging and type specimens (Gerringer et al. 2017a). Recent molecular studies have uncovered systematic issues within the Liparidae, with multiple described clades such as *Careproctus* and *Paraliparis* Collett, 1879 being polyphyletic (Orr et al. 2019). Further, *Notoliparis* and *Pseudoliparis*, while geographically isolated, are closely related both morphologically and genetically and should likely be synonymized (Gerringer et al. 2017a; Orr et al. 2019).

In 2018, one specimen of an undescribed hadal liparid was collected from 6714 m depth by a baited trap in the Atacama Trench, southeast Pacific Ocean. Cameras recorded two additional hadal snailfish species with distinct morphologies between 5920 and 7608 m. The collected individual is only the second hadal liparid recovered in this region, the first being *N. antonbruuni*. Herein, we describe this species as *Paraliparis selti* sp. nov. using a combined morphological and molecular taxonomic approach. We show that this species belongs to the genus *Paraliparis* and represents an independent evolutionary lineage in the hadal zone, distinct from all currently described hadal snailfishes.

## Materials and methods

### Sampling

As part of the HADES-ERC (European Research Council) project, cruise SO261 on the RV *Sonne* in March 2018, two identical free-fall landers were deployed 18 times between the depths of 2537 and 8052 m (Table 1; Fig. 1; full deployment list in Supplementary Table 1). The landers were equipped with purpose-built high-definition cameras and LED lighting. The cameras were powered by a 12V lead-acid battery (SeaBattery, Deep Sea Power and Light, San Diego, CA). Thirty second recordings were taken every 1.5 min, with an 8 megapixel still image taken between videos. Pressure and temperature were recorded at 30-s intervals using a separate sensor (RBRDuet; RBR Ltd, Canada). Specimens were collected using acrylic cylinders 20 cm in diameter and 100 cm long with inverted funnel entrances of 5-cm diameter. The cameras and traps were baited with locally sourced mackerel (Scombridae).

Additional snailfish species observed by in situ filming, without voucher specimens, are referred to by their morphotype and site locator tag as used in Jamieson et al.

**Table 1** Lander deployments where snailfishes were observed arranged by increasing depth in meters. Latitude and longitude are given in decimal degrees. Snailfishes were not observed at deployments shallower than 5920 m or deeper than 7608 m. Snailfish observations are presented as  $N_{\max}(T_{\text{arr}})$ , where  $N_{\max}$  is the maximum number observed in the same

frame and  $T_{\text{arr}}$  is the first arrival time in minutes following lander touchdown. Data in bold denotes the deployment the holotype was captured. Morphotype names of the other snailfish follow Jamieson et al. (2021)

Lat	Long	Depth	<i>P. selti</i> sp. nov.	Liparid sp. indet. 2-PCT	Liparid sp. indet. 3-PCT
5563 and shallower — not observed					
−20.34347	−71.12135	5920	1 (316)	1 (972)	
−20.34350	−71.13040	6025	1 (907)	1 (731)	
−21.72033	−71.26355	6520	1 (499)	1 (211)	1 (137)
−21.74162	−71.25775	6714	<b>2 (278)</b>	3 (676)	1 (54)
−23.05025	−71.23322	6974		1 (838)	1 (184)
−23.04997	−71.25073	7139			2 (800)
−23.37307	−71.39295	7204	1 (90)		
−23.83300	−71.34392	7493	1 (569)		1 (316)
−23.82900	−71.34633	7608	1 (854)		
7834 and deeper — not observed					

(2021) based on the open nomenclature (ON) qualifiers as described in Sigovini et al. (2016) and video-based classification standardisation as described in Horton et al. (2021).

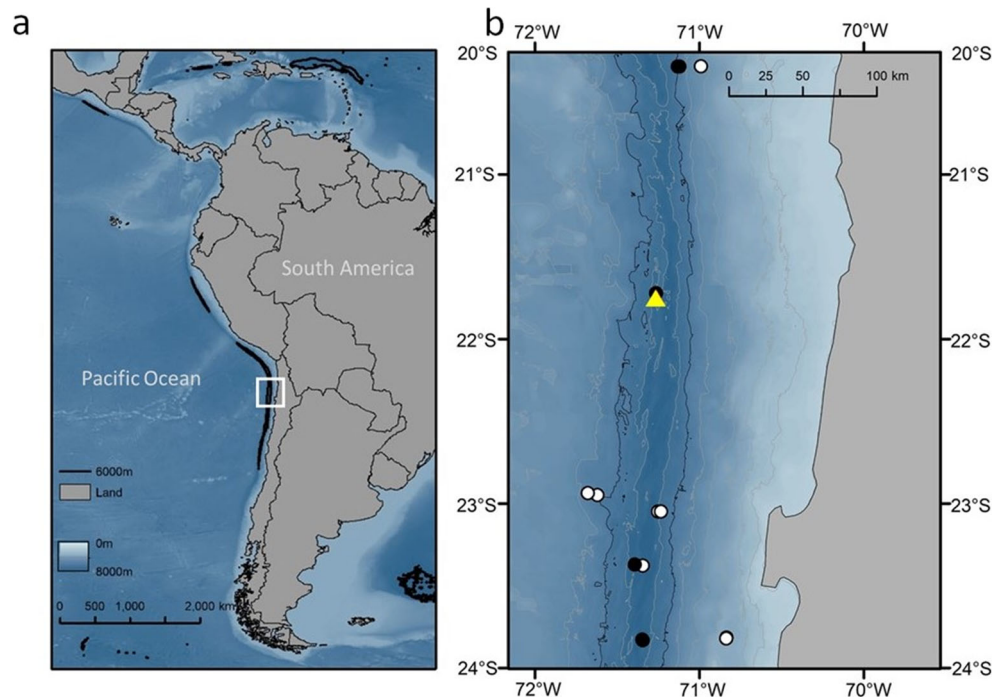
### Holotype processing

Upon collection, the holotype was immediately put on ice and transferred to a 4°C cold room for processing. Two fin-clips were taken from the distal portion of the right pectoral fin and preserved in 95% ethanol for genetic analysis. The specimen

was photographed in an aquarium containing chilled seawater using a Canon EOS750D and Tamron 90 mm F/2.8 macro lens with a Hoya polarising filter.

The holotype was fixed in 4% buffered formalin for 4 months, before being transferred to 75% ethanol for final storage. The specimen was transitioned to ethanol with 24-h soak periods in freshwater, 25% ethanol, and then 50% ethanol. The right pectoral girdle was dissected (preserving the left side intact) and stained using alizarin red S and alcian blue (Fisher Scientific) (Taylor 1967; Dingerkus and Uhler 1977).

**Fig. 1** **a** Atacama Trench along the west coast of South America, where the white box indicates the position of **b**. **b** Locations of lander deployments. White dots represent sites where *P. selti* sp. nov. was not observed, the black dots are where *P. selti* sp. nov. was observed, and the yellow triangle indicates where the holotype was recovered. The 6000 m depth contour marking the hadal zone is shown in black in **a** and **b**, and 1000 m isobaths are shown in grey in **b**. Bathymetric data from GEBCO (2015)



Post-preservation images were taken using the same photographic equipment with Helicon Remote and processed as an image stack using Helicon Focus (HeliconSoft 2017). The holotype was imaged using X-ray micro-computed tomography (micro-CT) at the Natural History Museum, London, using a Nikon Metrology HMX ST 225 (Nikon metrology Europe NV, Leuven, Belgium) with a tungsten reflection target head. Experimental conditions comprised a source voltage of 90 kV and current of 111 A using a 0.5-mm aluminium filter; the object-detector distance of 58.7 mm and the source-detector distance of 1115.1 mm generated data with a voxel resolution of 10.0  $\mu\text{m}$ . As the specimen was not fitting in the vertical field of view with the magnification setting, 5 acquisitions were necessary, moving the sample with the motorised manipulator on the vertical axis. Each acquisition consisted of 3142 projections of 1415 msec exposure each, with a frame averaging of 2. Each individual acquisition was reconstructed using CT pro 3D 3.1 (Nikon metrology Europe NV, Leuven, Belgium), generating 32-bit volume. All 5 acquisitions were merged following the protocol described in Butler et al. (2022) and exported as a single stack of 16-bit tiff images. To improve the signal-to-noise ratio and reduce file size, the dataset was reduced with a  $2 \times 2 \times 2$  binning. Hypural plate and posterior fin rays were also observed using a Leica DMi8 inverted microscope and DFC295 camera.

The morphological description follows Stein et al. (2001), cephalic sensory pore series are given as nasal, infraorbital, preoperculomandibular, and temporal (postorbital and suprabranchial). Vertebral counts are given as abdominal and caudal vertebrae (urostyle included). Abbreviation for counts and measurements follow Stein and Chernova (2002). Museum abbreviations follow Sabaj (2016).

Type material is deposited at the Museo Nacional de Historia Natural, Santiago, Chile (MNHNCL ICT 76227).

### DNA extraction and PCR amplification

To support the description of this species, we applied an integrative taxonomic approach that included analysis of three mitochondrial barcoding regions, 16S rRNA (16S), cytochrome oxidase I (COI), and cytochrome b (Cyt-b). Total genomic DNA was extracted from a fin clip of the single individual of *P. selti* sp. nov. using a standard phenol-chloroform approach. The three partial mitochondrial genes were amplified using published primers sets (Supplementary Table 2). PCR reaction mixes contained 0.2mM each dNTPs, 2.5mM  $\text{MgCl}_2$ , 0.5 $\mu\text{M}$  each primer, 0.5U of Taq DNA polymerase (Bioline), 10ng DNA template in  $1 \times \text{NH}_4$  buffer (Bioline) in a total reaction volume of 20 $\mu\text{l}$ . PCR conditions were as follows: initial denaturation at 95°C for 2 min, followed by 35 cycles of denaturation at 95°C for 30s, annealing at 48°C (16S) or 52°C (COI, Cyt-b) for 30s, extension at 72°C for 1 min, before a final extension step at 72°C for 2 min. PCR

products were purified enzymatically using ExoSAP-IT® (USB, Cleveland, OH, USA) as described in Bell (2008) and quantified by direct comparison with lambda DNA size standards on a 2% TBE agarose gel. Sequencing was undertaken with an ABI 3730xl automated DNA sequencer (MWG Eurofins, Germany).

### Phylogenetic analyses

With the three barcoding markers, we constructed three datasets to infer the genetic relationship of *P. selti* sp. nov. to other snailfishes. Due to the absence of *Paraliparis* species with publicly available 16S and Cyt-b sequences, we largely focused on a COI dataset to investigate the placement of *P. selti* sp. nov. within the Liparidae. The Liparidae COI dataset (605 bp) comprised of the 56 species of *Careproctus*, *Elassodiscus*, *Liparis*, *Paraliparis*, *Pseudoliparis*, *Nectoliparis*, *Notoliparis*, and *Rhinoliparis* with available sequence data (Table 2). Lumpfish (Family Cyclopteridae Bonaparte, 1831) are a commonly used outgroup for Liparidae phylogenies due to their close relationship with the family (Gerringer et al. 2017b; Orr et al. 2019). Here, we selected the smooth lumpfish, *Aptocyclus ventricosus* (Pallas, 1769), as the outgroup. In addition to the Liparidae COI dataset, we constructed two datasets for all snailfish species with available sequence data at each loci (16S, COI, Cyt-b, and concatenated). The first dataset comprised of a reduced sequence length with 10 Liparidae species, and the second dataset comprised the full sequence length with six Liparidae species. The methods and phylogenies constructed for other loci are presented in the [Supplementary Information](#).

Electropherograms were viewed in MEGA X (Kumar et al. 2018) where primer sequences and any ambiguous bases were trimmed. Sequence identity was confirmed using NCBI BLASTn (Altschul et al. 1990). Nucleotide sequences for COI and Cyt-b were translated into amino acid sequences to check for the presence of stop codons. Nucleotide alignments were constructed on the webPRANK server (Löytynoja and Goldman 2010) and confirmed by eye. The optimal evolutionary model for each dataset was identified by jModelTest 2.1.6 (Darriba et al. 2012) using both the Akaike information criterion (AIC) and the Bayesian information criterion (BIC). Both AIC and BIC identified the same best-fit models for the Liparidae COI dataset, Tamura and Nei 1993 model with gamma distribution and proportion of invariable sites (TN93+G+I) (Kimura 1981; Hasegawa et al. 1985; Tamura and Nei 1993).

Topologies were inferred using both maximum-likelihood and Bayesian approaches using PhyML v.3.1 (Guindon et al. 2010) and the Bayesian evolutionary analysis by sampling trees (\*BEAST) software package v1.10.4 (Suchard et al. 2018), respectively. Maximum-likelihood analyses were

**Table 2** GenBank accession numbers and references for all samples included in the analysis of the COI barcoding gene. Identifications reflect those updated in Orr et al. (2019), different identifications on GenBank are in brackets. Asterisks denote unpublished data. The species depth ranges were compiled from FishBase and cross-referenced using primary literature

	GenBank accession number	GenBank reference	Depth range (m)	Depth reference
<b>Family: Cyclopteridae</b>				
<i>Aptocyclus ventricosus</i>	AP004443	Miya et al. (2003)	0–1700	Solomatov and Orlov (2018) Orr et al. (2020)
<b>Family: Liparidae</b>				
<i>Careproctus longifilis (attenuates)</i>	FJ164428	Steinke et al. (2009)	1900–3334	Chemova et al. (2004)
<i>Careproctus canus</i>	FJ164432	Steinke et al. (2009)	244–434	Chemova et al. (2004)
<i>Careproctus continentalis</i>	HQ712898	Dettai et al. (2011)	425–600	Chemova et al. (2004)
<i>Careproctus cypselurus</i>	KY570326	Elz et al.*	35–1993	Orlov and Takranov (2011)
<i>Careproctus cypselurus (furcellus)</i>	FJ164447	Steinke et al. (2009)	35–1993	Orlov and Takranov (2011)
<i>Careproctus georgianus</i>	KX675940	Mabragaña et al. (2016)	85–285	Chemova et al. (2004)
<i>Careproctus gilberti</i>	JQ354029	Elz et al.*	172–886	Chemova et al. (2004)
<i>Careproctus longipectoralis</i>	HQ712900	Dettai et al. (2011)	2025–2037	Chemova et al. (2004)
<i>Careproctus melanurus</i>	GU440262	Hastings and Burton*	50–2453	Orr et al. (2020)
<i>Careproctus rastrinus</i>	JF952697	Zhang and Hanner (2011)	120–913	Chemova et al. (2004)
<i>Careproctus reinhardti</i>	HQ712338	Mecklenburg et al. (2011)	200–1000	Chemova et al. (2004)
<i>Elassodiscus caudatus</i>	GU440308	Hastings and Burton*	335–1040	Chemova et al. (2004)
<i>Liparis agassizii</i>	HM180656	Kim et al. (2012)	0–86	Chemova et al. (2004)
<i>Liparis atlanticus</i>	KC015556	McCusker et al. (2013)	0–90	Chemova et al. (2004)
<i>Liparis bathyarccticus</i>	HQ712568	Mecklenburg et al. (2011)	400–647	Chemova (2008)
<i>Liparis dennyi</i>	KY570339	Elz et al.*	73–225	Chemova et al. (2004)
<i>Liparis fabricii</i>	HQ712555	Mecklenburg et al. (2011)	300–1800	Chemova et al. (2004)
<i>Liparis florum</i>	GU440375	Hastings and Burton*	0–10	Chemova et al. (2004)
<i>Liparis fucensis</i>	GU440376	Hastings and Burton*	10–338	Chemova et al. (2004)
<i>Liparis gibbus</i>	AM498312	Byrkjedal et al. (2007)	30–647	Chemova et al. (2004)
<i>Liparis liparis</i>	KJ204977	Knebelberger et al. (2014)	3–78	Chemova et al. (2004)
<i>Liparis montagui</i>	KJ128532	Bergsten et al.*	0–30	Chemova et al. (2004)
<i>Liparis dennyi (mucosus)</i>	JQ354182	Elz et al.*	0–15	Chemova et al. (2004)
<i>Liparis ochotensis</i>	MG718032	Sim et al.*	58–761	Chemova et al. (2004)
<i>Liparis pulchellus</i>	JQ354185	Elz et al.*	9–183	Chemova et al. (2004)
<i>Liparis rutteri</i>	JQ354186	Elz et al.*	0–73	Chemova et al. (2004)
<i>Liparis tanakae</i>	JF952785	Zhang and Hanner (2011)	50–121	Chemova et al. (2004)
<i>Liparis tunicatus</i>	HQ712583	Mecklenburg et al. (2011)	0–150	Chemova et al. (2004)
<i>Paraliparis antarcticus</i>	KX676116	Mabragaña et al. (2016)	300–782	Chemova et al. (2004)
<i>Paraliparis bathybius</i>	EU326411	Rock et al. (2008)	1080–2824	Chemova et al. (2004)
<i>Paraliparis calidus</i>	KY033936	Kennington et al. (2017)	150–732	Chemova et al. (2004)
<i>Paraliparis cephalus</i>	KY570349	Elz et al.*	294–1799	Chemova et al. (2004)
<i>Paraliparis charcoti</i>	HQ713138	Dettai et al. (2011)	460–793	Chemova et al. (2004)
<i>Paraliparis copei</i>	KY033937	Kennington et al. (2017)	200–1692	Chemova et al. (2004)
<i>Paraliparis dactylosus</i>	FJ164953	Steinke et al. (2009)	541–1000	Chemova et al. (2004)
<i>Paraliparis leobergi</i>	HQ713145	Dettai et al. (2011)	165–970	Chemova et al. (2004)
<i>Paraliparis macropterus (aff. longipectoralis)</i>	JN641070	Smith et al.*	1133–1954	Stein (2012)
<i>Paraliparis mawsoni</i>	HQ713150	Dettai et al. (2011)	735–1080	Chemova et al. (2004)
<i>Paraliparis megalopus (melanobranchus)</i>	FJ164959	Steinke et al. (2009)	2830–3585	Chemova et al. (2004)
<i>Paraliparis neelovi</i>	JN641069	Smith et al.*	1070–2000	Chemova et al. (2004)
<i>Paraliparis paucidens</i>	FJ164964	Steinke et al. (2009)	1536–2275	Chemova et al. (2004)
<i>Paraliparis pectoralis</i>	GU440448	Hastings and Burton*	681–1536	Chemova et al. (2004)
<i>Paraliparis rosaceus</i>	KY570351	Elz et al.*	1050–3358	Chemova et al. (2004)
<i>Paraliparis operculosus</i>	JN640730	Smith et al. (2012)	380–1010	Chemova et al. (2004)
<i>Paraliparis</i> sp. BOLD:AAB1886	FJ164985	Steinke et al. (2009)	2250–2250	Steinke et al. (2009)
<i>Paraliparis</i> sp. MOP110189	MF956930	Robertson et al. (2017)	153–176	Robertson et al. (2017)
<i>Paraliparis</i> sp. JRAS06-106	EU326410	Rock et al. (2008)	n/a	
<b><i>Paraliparis selti</i> sp. nov.</b>	<b>MN422493</b>	<b>This paper</b>	5913–7616	<b>This paper</b>
<i>Paraliparis thalassobathyalis</i>	EU326328	Rock et al. (2008)	620–1600	Chemova et al. (2004)
<i>Paraliparis valentinae</i>	HQ713151	Dettai et al. (2011)	841–1100	Chemova et al. (2004); Dettai et al. (2011)
<i>Pseudoliparis belyaevi</i>	-	T.P. Satoh, Pers. Comm.	6380–7703	Gerringer (2019)

**Table 2** (continued)

	GenBank accession number	GenBank reference	Depth range (m)	Depth reference
<i>Pseudoliparis swirei</i>	KY659185	Gerringer et al. (2017b)	6198–8178	Gerringer (2019)
<i>Nectoliparis pelagicus</i>	FJ164909	Steinke et al. (2009)	200–3383	Chemova et al. (2004)
<i>Notoliparis kermadecensis</i>	KY659180	Gerringer et al. (2017b)	5879–7669	Linley et al. (2016)
<i>Notoliparis stewarti</i>	KY659178	Gerringer et al. (2017b)	6456–7560	Stein (2016)
<i>Rhinoliparis attenuatus</i>	FJ165100	Steinke et al. (2009)	350–2189	Chemova et al. (2004)
<i>Rhinoliparis attenuates (barbulifer)</i>	GU440505	Hastings and Burton*	350–2189	Chemova et al. (2004)
<i>Rhinoliparis attenuatus</i> (sp. 1)	KF918899	Elz et al.*	350–2189	Chemova et al. (2004)

conducted with a neighbour-joining starting tree and using nearest neighbour interchange branch swapping using the model of sequence evolution estimated by JModelTest2 but with the parameters estimated by PhyML. The stability of nodes was assessed from bootstrap support based upon 10,000 iterations. Bayesian analyses were run for 40,000,000 generations and sampled every 100,000 trees with an uncorrelated relaxed clock (Drummond et al. 2006). The respective models of sequence evolution estimated by jModelTest2 were used but with the parameters estimated by \*BEAST. Two independent runs were performed, and outputs were assessed with Tracer v1.7 to ensure convergence (effective sample size (ESS) >200). The two independent runs were combined in LogCombiner v1.8.4. with TreeAnnotator v1.8.4, the first 4,000,000 trees were discarded as burn-in where the partition frequencies among the remaining trees gave the posterior probabilities used to provide an estimate of clade credibility. Trees were visualised using FigTree v1.4.3 (Rambaut 2012) and annotated using Inkscape 0.92.2 (The Inkscape Team 2017).

We paired the Liparidae COI phylogeny with species depth ranges to evaluate depth relationships between clades (Table 2). The species depth ranges were compiled from FishBase (Froese and Pauly (2021) and checked in the primary literature (Chemova et al. 2004; Chernova 2008; Steinke et al. 2009; Dettai et al. 2011; Orlov and Tokranov 2011; Stein 2012; Linley et al. 2016; Stein 2016; Robertson et al. 2017; Solomatov and Orlov 2018; Gerringer 2019; Orr et al. 2020). While the species used within the Liparidae COI dataset are a good representation of known snailfishes, the absence of deep abyssal species is most likely an artefact of reduced sampling effort at these depths (Gerringer 2019).

## Results

### Systematics

#### Order Perciformes

#### Family Liparidae Gill, 1861

#### Genus *Paraliparis* Collett, 1879

#### *Paraliparis selti* Linley, Gerringer & Canto-Hernández\*, 2022, sp. nov.

\*Species authority, the current paper leverages a wide skillset reflected in the author list.

<https://zoobank.org/75003de2-4283-40d7-818c-8b4d0b43bd18>

(Figures 2, 4, 5, 6 and 7, 9, Supplementary 1–4)

*Paraliparis* sp. nov. — Jamieson et al. (2021): page 7, Figure 6, Table 6

**Common name** — Blue Atacama snailfish

#### **Material examined**

**HOLOTYPE** — MNHNC ICT 76227, 76 mm standard length, juvenile, Atacama Trench, 21.74162 °S, 71.25775 °W, 6714 m depth, RV *Sonne*, cruise SO261, 24th March 2018 (Fig. 2).

#### **Diagnosis**

We place *P. selti* sp. nov. within the genus *Paraliparis* based on the following characteristics: ventral disk absent, pseudobranchs absent, single pair of nostrils present, single suprabranchial pore present, coronal pore absent (Stein 2012), and six branchiostegal rays present (Kai et al. 2020). Lower pectoral fin lobe does not form a single filament. The hypural plate is not divided and is fused with the terminal vertebral column. The head lacks barbels or head flaps.

It differs from its congeners through a complex of characters; high number of vertebrae (65) particularly the abdominal vertebrae (12), dorsal fin rays (60), anal fin rays (52), and caudal fin rays (8); comparatively low number of pectoral fin rays (18) which forms a deep notch with two widely spaced non-rudimentary rays; mouth horizontal; Jaw teeth simple and not uniserial; colour in life, blue-black anteriorly becoming pale posteriorly, blue pigment becoming dusky when preserved, peritoneum black.

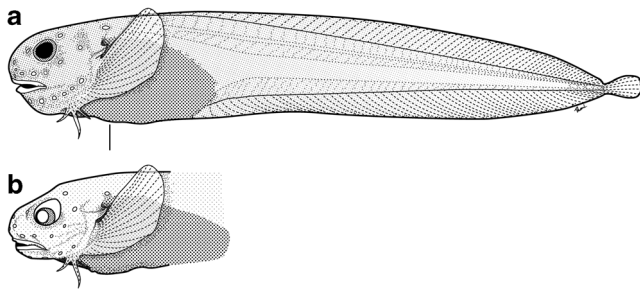


**Fig. 2** *Paraliparis selti* sp. nov. holotype, 6714 m, Atacama Trench. 83 mm total length, 75.9 mm standard length. **a** Freshly recovered. **b** Changes to anterior profile following preservation in 4% buffered formaldehyde and transfer to 75% ethanol

## Description

**Counts and proportions:** Dorsal rays 60, Anal rays 52, Vert 65 (12+53), pores; nasal 2, infraorbital 5, preoperculomandibular 7, temporal 2 (1 postorbital and 1 suprabranchial). Caudal rays 8. Branchiostegal rays 6 each side. Pelvic disk absent (Table 3). Head wide (HW, 14% SL) and moderately deep (HD, 14% SL, 88% HL). Body low (bd, 18% SL). Predorsal length short (preD, 17% SL). Anus to anal fin long (aAf, 34% SL). Upper pectoral-fin lobe long (UPL, 14% SL). Eye large (E, 4% of SL, 25% of HL). Interorbital width broad (io, 11% of SL, 68% of HL). Lower jaw short (lj 6% of SL, 39% of HL; Table 4).

**Head:** Snout is deep, rounded, slightly projecting pre-preservation. Snout became bluntly rounded following preservation (Fig. 2, Fig. 3). Subrostral fold is present but does not cover the entire upper lip. The eye is low and does not touch the dorsal contour of the head. Sub-orbital distance long, 90% of the eye diameter to the closest part of the upper lip. The mouth is horizontal (upper jaw symphysis below the lower margin of the eye) and subterminal with the lower tooth plate behind the upper plate but strongly

overlapping (Fig. 4). The jaw is relatively deep. Oral cleft reaching below the centre of the eye. Teeth are caniniform with the larger teeth towards the inside of the mouth. Premaxillary with prominent symphysis, in 8 rows of upwards of 9 teeth (Fig. 5a, Supplementary Figure 2). The mandibular tooth rows are less distinct (Fig. 5b). Dorsal pharyngeal jaw with well-developed teeth appearing to come together vertically in a rocking motion (Fig. 5c), a ventral pharyngeal jaw was not found and is not visible in Fig. 5 (Supplementary Figure 3). Six branchiostegal rays on each side, anterior two spaced from blade-like posterior rays. Pore-like single nostrils, level with the upper margin of the pupil. Pores are large, nasal pores 2, infraorbital pores 5, preoperculomandibular pores 7, temporal pores 2 (comprising 1 postorbital and 1 suprabranchial pore). Coronal pore is absent. Two oval chin pores are present, opening directly and separately on the skin surface with a crescent-shaped skin fold anteriorly but not extending posterior of the pores, interspace slightly wider than pore width, and unpigmented. The lateral chin profile is slanted at roughly 45°. Gill opening is restricted, completely above the pectoral fin, and covered by the opercular flap. The opercular flap is triangular with a blunt tip and moderate dorsally notched anterior base (Fig. 4).

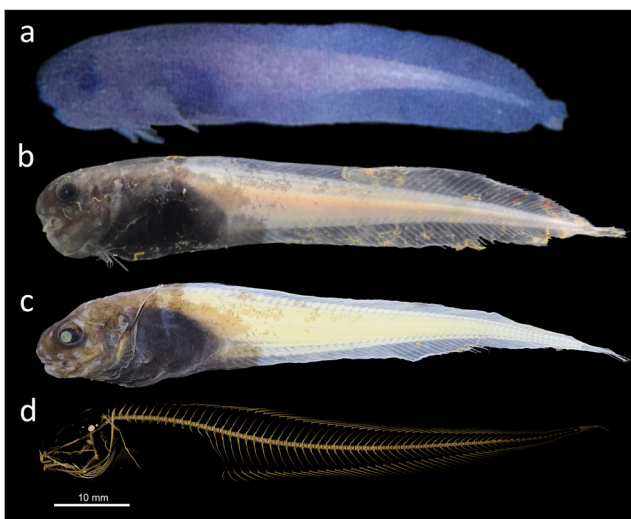
**Body:** The dorsal-most pectoral fin ray is in line with the ventral edge of the orbit. Upper pectoral fin lobe rays gradually decrease in length. There are no rudimentary pectoral fin rays, with 13 upper lobe rays, 2 notch rays, and 3 lower lobe rays. The pectoral girdle is long, extending almost to the mandibular symphysis (Fig. 4b). Rays of the upper pectoral fin lobe are close dorsally, becoming increasingly widely spaced following the 10th ray. The pectoral fin notch is wide with two equally spaced notch rays. The first ray of the lower pectoral fin lobe is twice as far from the second as the second is from

**Table 3** Counts for *P. selti* sp. nov. and the similar species *P. orcadensis* Matallanas & Pequeño, 2000 and *P. mawsoni* Andriashev, 1986

Counts	<i>P. selti</i> sp. nov.	<i>P. orcadensis</i>	<i>P. mawsoni</i>
Total vertebrae	65 (12+53)	-	67–71
Abdominal vertebrae	12	-	
Dorsal fin rays	60	68	61–65
Anal fin rays	52	60	55–60
Head pores			
Nasal	2	2	
Infraorbital	5	5	
Preoperculomandibular	7	7	
Temporal	2	2	
Total pectoral rays	18	19	23–24
Pectoral fin rays (upper lobe)	13	13	16–17
Pectoral fin rays (notch)	2	3	3–4
Pectoral fin rays (lower)	3	3	3–4
Total caudal fin rays	8	8	-

**Table 4** Morphometric details for *P. selti* sp. nov. Proportions given in per cent of standard length (SL) and head length (HL)

Measurement	Length (mm)	Ratio (%) of SL	Ratio (%) of HL
Total length (TL)	83	109.5	681.2
Standard length (SL)	76	100.0	622.1
Head length (HL)	12	16.1	100.0
Anus to anal fin origin (aAf)	26	34.0	211.5
Maximum body depth (bd)	14	18.1	112.3
Body depth at anal-fin origin (bdA)	11	14.0	86.9
Eye horizontal diameter (E)	3	4.1	25.4
Length of gill opening (go)	2	2.1	13.1
Head depth (HD)	11	14.1	87.7
Head width (HW)	10	13.6	84.4
Interorbital width (io)	8	10.9	68.0
Horizontal orbital width	4	4.6	28.7
Postorbital head length (po)	6	7.5	46.7
Suborbital distance	3	3.4	21.3
Upper jaw length (uj)	5	7.0	43.4
Lower jaw length (lj)	5	6.2	38.5
Lower pectoral fin lobe length (LPL)	5	6.3	39.3
Upper pectoral fin lobe length (UPL)	11	14.1	87.7
Length of shortest notch ray (NL)	1	1.6	9.8
Distance between lower pectoral fin lobes	4	4.7	29.5
Mandible symphysis to anus (ma)	10	13.6	84.4
Mandible to end of abdominal cavity	25	33.1	205.7
Pectoral symphysis to end of abdominal cavity	14	18.6	115.6
Pre-anal fin length (preA)	26	34.0	211.5
Pre-dorsal fin length (preD)	13	17.0	105.7
Snout (sn)	4	5.4	33.6
Snout to anus	11	14.5	90.2

**Fig. 3** Lateral view of *P. selti* sp. nov. MNHNC ICT 76227. **a** In situ at 6714 m (the deployment of recovery, 21.74162 °S, 71.25775 °W); **b** freshly recovered; **c** post-preservation in ethanol; **d** 3D rendering of the X-ray micro-CT data. The scale bar represents 10 mm

the third (Fig. 6). The rays of the lower pectoral fin lobe have more segments (5) than those of the notch (2). The number of segments in the intact upper lobe rays is unknown. Dorsal and anal fin pterygiophores present to at least the last three vertebrae. Hypural plate fused but with a visible cleft between the plates. Twelve abdominal vertebrae, the anterior most two lacking haemal arches, last three with short haemal spines but distinct from the much longer haemal spines of the 53 caudal vertebrae. No pleural ribs. The first dorsal ray inserts between the neural spines of the 5th and 6th vertebrae, one or two interneuralia (free pterygiophors) are between vert 4 and 5 (Fig. 3d, Supplementary Figure 1). The anus is in line with the posterior edge of the opercular spine.

**Colouration:** Body blue-black anteriorly becoming cream posteriorly in life. Peritoneum black. Skin partially transparent and subdermal extracellular matrix present but thin, potentially due to immaturity based on in situ observations of this morphotype. Preserved specimen dusky to anal fin origin, body pale in alcohol with black peritoneum (Fig. 3a).



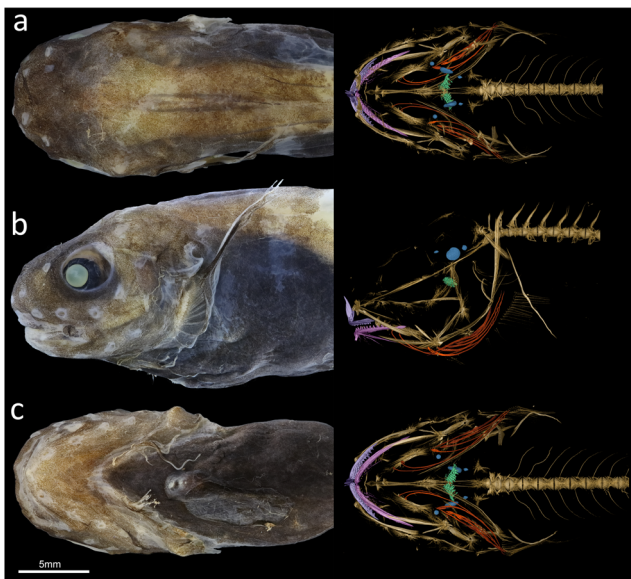


**Fig. 4** Anterior morphology of preserved *P. selti* sp. nov. MNHNC ICT 76227, external left, internal micro-CT scan structure right: **a** dorsal, **b** lateral, and **c** ventral surfaces. Oral jaws (premaxilla and dentary) are highlighted in lilac, upper pharyngeal jaws in green, otoliths (sagittae large, lapilli, and asterisci also shown) in blue, and branchiostegal rays in red. Some low-density bone structures such as the neurocranium are present in the specimen but not shown at this density threshold. The scale bar represents 5 mm

Only a single round dorsal radial was observed (Fig. 6). However, the ventral radials are often reduced in *Paraliparis* (Andriashev 1998) and the absence of calcification of the radials may prevent them from being visible following clearing and staining (Stein 2005). As there is some doubt as to if all radials have been observed, the number and position of them will not form part of the diagnosis. Fenestrae are not present and are rare within the genus (Orr et al. 2019). Distal radials were also not observed, consistent with other *Paraliparis* species (Orr et al. 2019).

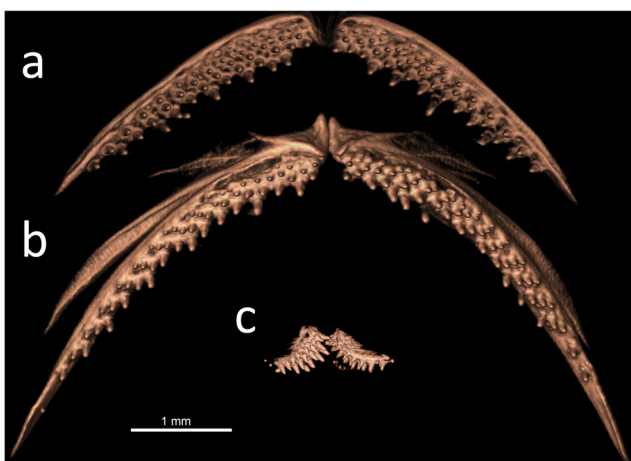


**Fig. 5** 3D rendering of the dentition in *P. selti* sp. nov. MNHNC ICT 76227 from CT data. **a** upper premaxillary; **b** lower dentary bone; **c** upper pharyngeal teeth. The density threshold has been adjusted in each to provide maximum detail. The scale bar represents 1 mm

## Distribution

Known only from the Atacama Trench (Fig. 1) between 5913 and 7616 m depth.

## Etymology

Named for “selti”, meaning blue in the almost extinct Kunza language of the indigenous peoples of the Atacama Desert. The waters over the Atacama Trench are especially productive, due in part to the mineral enrichment by dust deposits from this neighbouring Atacama Desert and aided by intense upwelling along the continental slope.

## Comparisons

In addition to its significantly deeper habitat in the Atacama Trench, *P. selti* sp. nov. can be distinguished from shallow-living south-eastern Pacific Ocean *Paraliparis* in having two widely spaced notch rays in the pectoral fin, with a total of 18 pectoral fin rays and a small and restricted gill opening positioned completely above the pectoral fin (Stein 2005). *Paraliparis selti* sp. nov. is also distinct from shallower *Paraliparis* from the west coast of Central and South America in having a horizontal mouth, rather than the oblique mouth of *P. debueni* Andriashev, 1986, *P. molinai* Stein et al., 1991, *P. angustifrons* Garman, 1899, and *P. membranaceus* Günther, 1887. Of the deeper-living Pacific *Paraliparis*, *P. selti* sp. nov. has fewer pectoral rays than *P. latifrons* Garman, 1899 (22); *P. fimbriatus* Garman, 1892 (24); *P. angustifrons* Garman, 1899 (37); *P. attenuatus* Garman, 1899 (24); *P. mawsoni* Andriashev, 1986 (23–24) and *P. plicatus* Stein, 2012 (21). It also has fewer pectoral fin rays than are known from Australian *Paraliparis* (Stein et al. 2001). It has slightly more than *P. thalassobathyalis* Andriashev, 1982 (15–17) but is best separated from *P. thalassobathyalis* by having more caudal rays (8 vs. 5). *Paraliparis selti* sp. nov. has similar counts and proportions to the North Atlantic’s *P. calidus* Cohen, 1968 and *P. bathybius* (Collett, 1879) but differs from the former in having more abdominal vertebrae (12 vs. 10) and the latter by having fewer notch rays (2 vs. 3–4). *Paraliparis selti* sp. nov. is distinct from *P. paucidens* Stein, 1978 and *P. neelovi* Andriashev, 1982 in that *P. selti* sp. nov. does not have uniserial teeth on either jaw. *Paraliparis selti* sp. nov. also differs from genetically similar species in having fully developed pectoral notch rays, as opposed to the fully rudimentary notch rays of *P. garmani* Burke, 1912, *P. neelovi*, *P. voroninorum* Stein, 2012, *P. stehmanni* Andriashev, 1986, *P. longicaecus*, *P. camilarus*, *P. plicatus*, and *P. nullansa* Stein, 2012 and the singular or partial rudimentary rays of *P. posteroporus* and *P. parviradialis* Stein, 2012.

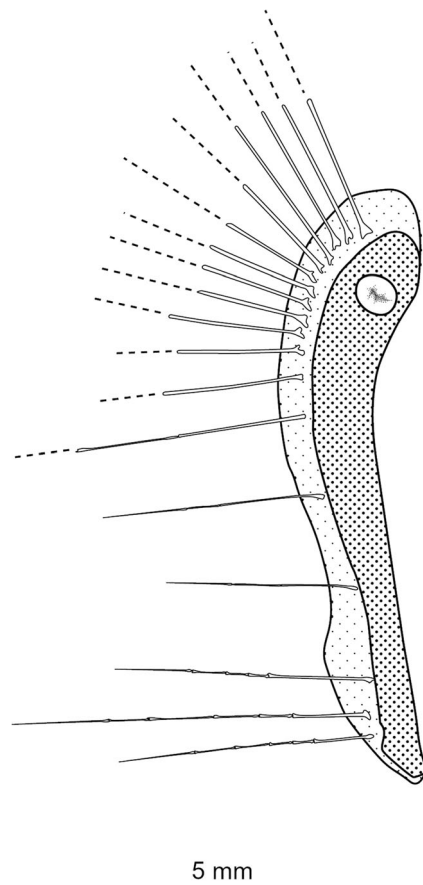
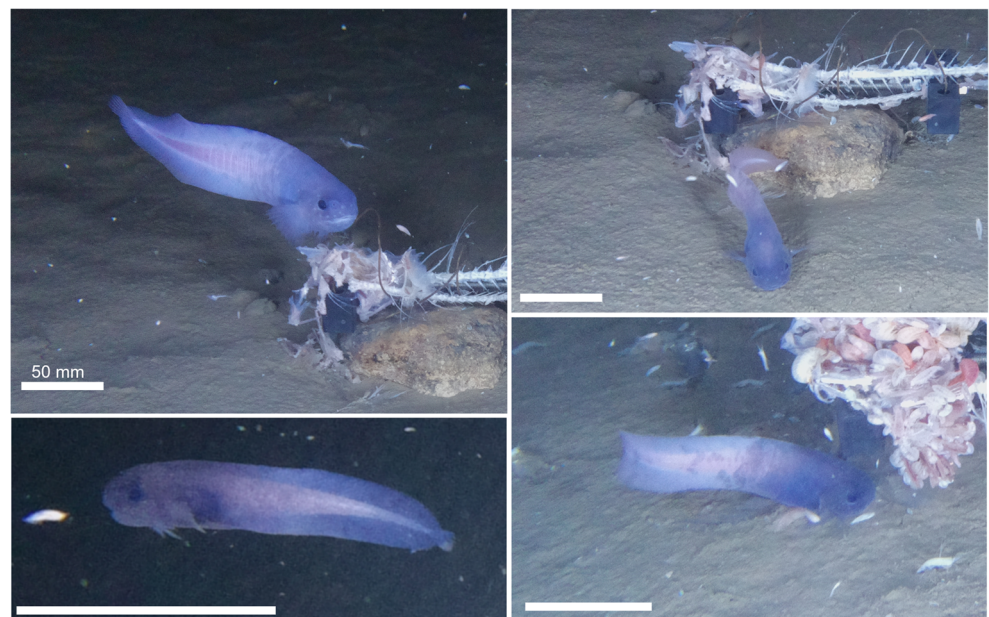


**Fig. 6** Pectoral girdle of *P. selti* sp. nov., medial view (right side - vertically flipped). The scale bar represents 5 mm

Morphologically, *P. selti* sp. nov. most strongly resembles Antarctic rather than Southern Pacific species. The relatively high counts for vertebrae, dorsal, and anal rays and a relatively

**Fig. 7** In situ still images of *P. selti* sp. nov. taken by baited camera. Upper row, 6520 m depth at  $-21.7203, -71.2636$  (Lat, Long); lower row, 6714 m depth at  $-21.7416, -71.2578$ . Scale bars 50 mm



low number of pectoral fin rays is common within what Andriashev (2003) called the long-tailed *Paraliparis*. *Paraliparis selti* sp. nov. most closely resembles the bathyal *P. orcadensis* Matallanas & Pequeño, 2000 but has fewer dorsal (60 vs. 68) and anal (52 vs. 60) fin rays, *P. orcadensis* is also described as uniform grey with nearly back snout and fins rather than *P. selti* sp. nov.'s variegated blue colour.

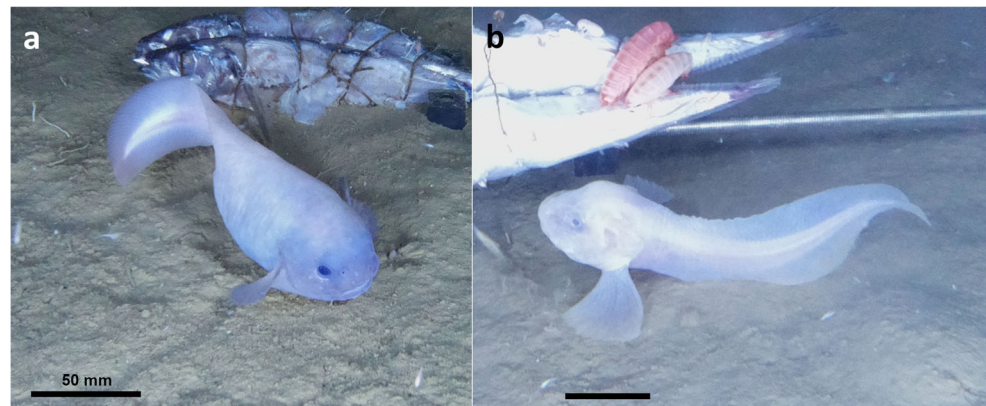
### Video observations

At upper trench depths (lander deployments from 5913 to 7616 m) the Atacama Trench ichthyofauna was dominated by three hadal snailfish morphs: *Paraliparis selti* sp. nov. (Fig. 7), *Liparide* sp. indet. 2-PCT, and *Liparid* sp. indet. 3-PCT, as reported in Jamieson et al. (2021) (Fig. 8, Supplementary Video 1, Supplementary Video 2).

In situ recording of *P. selti* sp. nov. showed a high degree of variation in size and colour/pattern. Generally, however, *P. selti* is deep blue anteriorly becoming pale posteriorly in a blotchy and irregular manner (Fig. 7). *Paraliparis selti* sp. nov. possessed the widest bathymetric range of the snailfishes observed, from 5920 to 7608 m. The arrival time ( $T_{arr}$ ) and maximum number ( $N_{max}$ ) suggest that *P. selti* sp. nov. are most abundant around 6700 m depth (Table 1). They appear attracted to the mackerel bait but would not feed on it, instead feeding on the gathered amphipod swarm. No features were observed that differentiated recordings of this morphotype from the collected specimen, which forms the holotype for *P. selti* sp. nov. described herein.

The two additional snailfish morphs recorded in situ but not collected possess features which distinguish them from *P. selti* sp. nov. *Liparid* sp. indet. 2-PCT is a larger and more

**Fig. 8** **a** Liparid sp. indet. 2-PCT 6025 m depth at  $-20.3435, -71.1304$  (Lat, Long); **b** Liparid sp. indet. 3-PCT at 6714 m depth at  $-21.7416, -71.2578$ . Scale bars 50 mm



robust morph. It is dusky pink in colour with a darker peritoneum visible through the fish's translucent skin (Fig. 8a). From the image data, it was possible to observe a well-developed ventral suction disk, a posterior anus near the anal fin origin, and a blunt and broad-based opercular spine. Photos also revealed that the pectoral fins of Liparid sp. indet. 2-PCT comprise at least 15+3+4 rays. The lower pectoral fin lobe rays are free and the tips of the notch rays are partially free. The notch is moderately deep with more widely spaced rays. The pectoral fins do not reach to the end of the peritoneum. The snout is short, about double the eye diameter, and the profile is rounded. The head and body are broad and gelatinous with thin and loose skin. This morph would often settle directly on the bait and suction feed on the amphipod swarm, becoming visibly engorged during the recordings.

The third snailfish morph seen in the Atacama Trench, Liparid sp. indet. 3-PCT, was easily distinguished by its large wing-like upper pectoral lobes, large head with small eyes, and prominent, sloped snout (Fig. 8b). This pale morph has been previously recorded in the Atacama Trench as 'unidentified liparid from 7050 m' in Jamieson (2015) and 'The Perú-Chile Snailfish' in Linley et al. (2016). The morphotype possesses at least 19+2+4 pectoral rays. The rays of the lower lobe are thick and free, curving slightly anteriorly. The rays of the notch are more widely spaced than those of the upper lobe; the notch is shallow and not clearly distinct from the lobes. The tips of the upper lobe and notch rays are free. The snout is prominent, and there is an abrupt change to the profile at the orbit. The centre line of the snout forms a ridge and may be due to an enlarged ethmoid (nasal) bone, as is found in the genus *Eknomoliparis*. The snout is more than five times the eye diameter. The body cavity is short, less than the head and pectoral fin lengths. This morph tended not to approach the bait as closely as the other morphotypes and would hunt amphipods in the periphery.

### Phylogenetic analyses

*Paraliparis selti* sp. nov. was successfully characterised across three gene amplicons where 1476 bp were resolved for 16S,

1399 bp for COI, and 1007 bp for Cyt-b. These sequences have been annotated and deposited into GenBank and can be accessed under GenBank accession numbers MN423252 for 16S, MN422493 for COI, and MN422494 for Cyt-b.

Phylogenetic inference within the COI phylogeny strongly supports the placement of *P. selti* sp. nov. within the genus *Paraliparis* (Fig. 9). *Paraliparis selti* sp. nov. is well-supported in a sub-clade with *P. mawsoni*, *P. paucidens*, *P. calidus*, and *P. neelovi* (1 Bayesian posterior probability, 97% ML bootstrap support). Within the available species, it is most closely related to *P. paucidens* and *P. calidus* (0.93 Bayesian posterior probability, 65% ML bootstrap support).

More broadly within the liparids, the COI phylogeny suggests that *Liparis* is monophyletic while both *Paraliparis* and *Careproctus* do not form monophyletic genera (Fig. 9). Instead, there are three distinct *Paraliparis* sub-clades, which are polyphyletic because of *Rhinoliparis*. *Careproctus* is split into two distinct lineages by *Paraliparis* and *Rhinoliparis*, with a clade of *C. attenuates*, *C. continentalis*, *C. georginus*, and *C. longipectolis* being sister to *Paraliparis*. Further, the larger COI gene topology resolves the placement of other hadal snailfishes, *Pseudoliparis* and *Notoliparis*, relative to *P. selti* sp. nov. While *P. selti* sp. nov. is firmly placed within the *Paraliparis*, *Pseudoliparis*, and *Notoliparis* are rooted basal to the *Careproctus*, *Paraliparis*, and *Rhinoliparis* lineages (0.9 Bayesian posterior probability, unsupported ML bootstrap support).

### Morphological characters of Clade M

The COI phylogenetic analysis (Fig. 9) placed *P. selti* sp. nov. within Clade M, as defined by Orr et al. (2019). Clade M is dominated by Antarctic species (14 of the 19 species), but surprisingly contains the Northern Atlantic species *P. garmani*; *P. bathybius* (Collett, 1879) and the Northern Pacific *P. paucidens* Stein, 1978; in addition to an undescribed species. They are all found deeper than ~600 m with most species captured ~1500–2000 m deep. The tooth shape is consistently simple (or unknown in two cases) but is dominated by uniserial tooth patterns

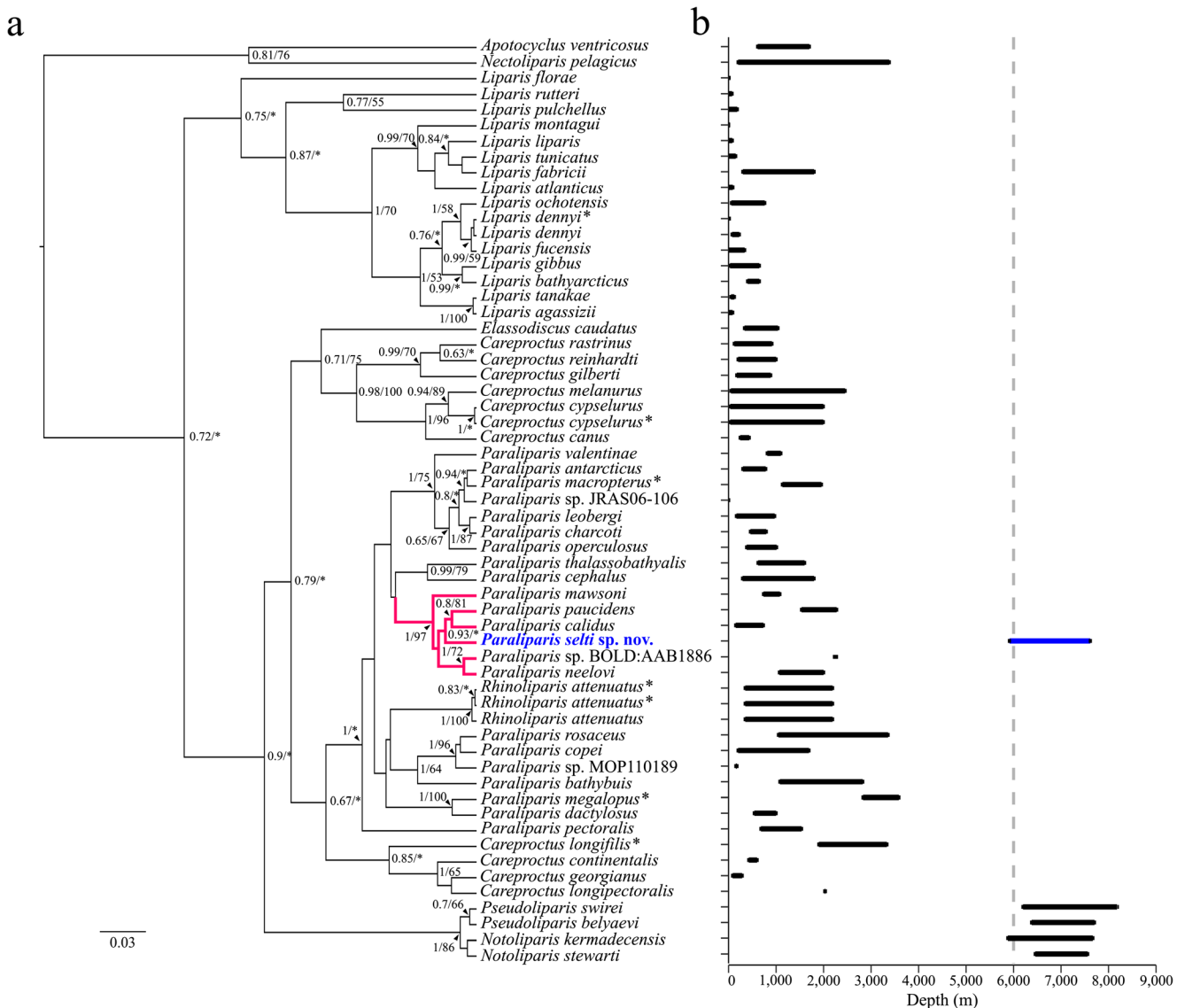


**Fig. 9** Bayesian tree showing the position of *P. selti* sp. nov. within the liparids using the COI barcoding region (a) with corresponding depth distributions compiled from FishBase and cross-referenced in the primary literature (b; Table 2). Bayesian posterior probabilities and Maximum-likelihood bootstrap supports are shown on branch nodes. Values less

than 50% or values not supported by the alternative method are not stated or depicted by an asterisk. Names with asterisks signify revised identifications by Orr et al. (2019). Clade M within the phylogeny, as defined by Orr et al. (2019), is represented by bolded pink lines

on at least one jaw, although many are bi-tri serial near the symphysis, e.g. *P. plicatus* Stein, 2012; *P. camilarus* Stein, 2012; *P. voroninorum*; *P. bathybius*; and *P. stehmanni*. The only exceptions are *P. selti* sp. nov. described herein and *P. mawsoni* who both have teeth arranged in bands. Stein (2012) felt that uniserial dentition likely evolved multiple times within the *Paraliiparis* and so may not indicate a common lineage, but uniserial teeth are undoubtedly a feature of Clade M. Most Clade M *Paraliiparis* have a horizontal subterminal or inferior mouth with the exceptions of *P. germani*'s oblique mouth and *P. bathybius*'s terminal mouth. Counts are very consistent within the clade, pectoral rays 18–25, vertebrae 65–71 with abdominal vertebrae always >10, dorsal rays 56–66, anal rays 51–56, caudal rays 7–8 (with some

exceptions: 6 in *P. voroninorum* and 6–8 in *P. paucidens*). Where reported, chin pores are paired. The gill opening is restricted, often completely above the pectoral fin. Orbit diameter is ~30% of head length. The morphological and genetic similarities within Clade M snailfishes raise the hypothesis of an Antarctic origin for this hadal radiation.

## Discussion

The discovery of *P. selti* sp. nov. between 5920 and 7608 m represents another endemic and ecologically important hadal snailfish (Fujii et al. 2010; Linley et al. 2016; Gerringer 2019;

Jamieson et al. 2021). Further, this species provides insights into the evolution of snailfishes into the deep sea. The paths taken in the radiation and colonisation of the snailfishes, particularly around the Pacific Americas and Australia, are still not resolved (e.g. Orr et al. 2019). Genetic data from rare South American Pacific Ocean species, such as *P. selti* sp. nov., will ultimately aid our understanding of how snailfishes have evolved, adapted, and diversified into the greater depths of the deep sea.

We applied molecular barcoding loci to examine the phylogenetic placement of *P. selti* sp. nov. within the Liparidae and confirmed its taxonomic placement based on morphology within the *Paraliparis* genus (Fig. 9). Mounting evidence strongly suggests that the genus *Paraliparis* is paraphyletic and in need of taxonomic revision (e.g. Kido 1988; Knudsen et al. 2007; Orr et al. 2019). Our molecular phylogenies support this assertion. Notwithstanding, our phylogenies did place *P. selti* sp. nov. within the main *Paraliparis* Clade M defined by Orr et al. (2019). Upon review, the members of Clade M possessed common traits. They were mostly found in the Antarctic at bathyal depths. Most show a reduction in dentition with uniserial simple teeth on at least one jaw. Counts were quite consistent, and they tended to be long-bodied, with high abdominal vertebrae counts. The inclusion of molecular data from multiple loci, such as those presented here, will help elucidate the phylogenetic relationships in *Paraliparis* and the family Liparidae overall. There is even mounting support for including the Liparidae within the separate Order Cottiforms, based on both morphological and molecular evidence (Imamura and Abe 2002; Wiley and Johnson 2010). To align with the currently accepted literature, we have continued to use Perciformes but acknowledge that Cottiforms should likely be adopted in the future.

The in situ behaviour of *P. selti* sp. nov. resembles that recorded for other hadal snailfishes (Fig. 7, Supplementary Video 3). *P. selti* sp. nov. are suction-feeding predators that prey on scavenging amphipods attracted to the bait (rather than a scavenger of the bait itself) consistent with other hadal snailfishes (Linley et al. 2016; Gerringer et al. 2017c; Linley et al. 2017). Amphipods were found within the holotype's buccal cavity upon recovery and the micro-CT data revealed its stomach contained many amphipods (Supplementary Figure 4). Strong pharyngeal jaws are prevalent within the hadal snailfishes and appear to be an adaptation to feeding on the abundant hadal amphipods (Gerringer 2019). Functional morphology and variation within liparid pharyngeal jaws, particularly in deep-sea representatives which tend to show a reduction in hard body parts, is well-worth continued study. With the continued adoption of techniques such as micro-CT, pharyngeal jaw morphology may become an important diagnostic character in the Liparidae and is likely to withstand the damage done by recovery and preservation.

Adaptive radiation of liparids into hadal trenches has been hypothesised to have occurred independently, with the hadal descent of an abyssal lineage in the northwest Pacific Ocean and a separate descent to the southwest Pacific Ocean (Priede and Froese 2013). In contrast, more recent genetic studies indicate that all previously known hadal snailfishes form a single clade, which is basal to other snailfishes (Gerringer et al. 2017b; Gerringer 2019; Orr et al. 2019), thus, more suggestive of a singular hadal lineage. The COI inferred phylogeny presented by this study strongly support a different case for *P. selti* sp. nov., which appears to represent an independent radiation into the hadal zone (Fig. 9; Supplementary Figure 5, 6). Those species genetically most closely related to *P. selti* sp. nov. are also predominantly from the Southern Ocean, where recent in situ observations by Jamieson et al. (2021) reported three hadal snailfish morphs very closely resembling those recorded in the Atacama Trench. Future research may reveal an Antarctic origin to this second independent radiation into the hadal zone. The singular specimen of *P. selti* sp. nov. may prove important to our understanding of both snailfish radiation and their adaptations to life at hadal depths.

## Conclusion

The snailfishes are among the most rapidly radiating families of marine fishes, resulting in a worldwide distribution from the coastal waters to the hadal trenches. Due to the challenges of sampling at depths >6000 m, the full diversity of snailfishes remains unresolved. *Paraliparis selti* sp. nov. represents an important new species which confirms a second and independent lineage of vertebrate life adapted to hadal depths. This progresses our understanding of the colonization and diversification of snailfishes into hadal trenches and the factors that allow this family to live in the ocean's deepest zones.

**Supplementary Information** The online version contains supplementary material available at <https://doi.org/10.1007/s12526-022-01294-0>.

**Acknowledgements** The holotype was obtained during the RV *Sonne* cruise SO261 (ship time provided by BMBF, Germany). We thank the captain, crew, and scientific personnel, specifically Heather Stewart (BGS) for their support in this work. The expedition was part of the HADES-ERC Advanced grant "Benthic diagenesis and microbiology of hadal trenches" grant (agreement number 669947) awarded to Ronnie N Glud (University of Southern Denmark). We thank Osvaldo Ulloa of the Instituto Milenio de Oceanografía, Universidad de Concepción (IMO-UdeC, Chile) for, on behalf of Chile, loaning us the specimen from their waters so that we may describe it. Thank you to Professor Rob Upstill-Goddard for travel funds. We thank Katherine Maslenikov (Burke Museum, University of Washington) for consultation on visualizing radials. We thank our reviewers for their time to greatly enhance this work through their detailed and constructive comments. Regarding access to comparative material, we are grateful to James Maclaine, Senior curator of fishes at the Natural History Museum,

London; Marcus Anders Krag and Peter Rask Møller of the Natural History Museum of Denmark. We thank Natalia Chernova of the Zoological Institute, Russian Academy of Sciences, and Sandra Raredon and Jeff Williams of the Smithsonian Institution for photographs, x-ray, and discussion of types when they were not possible to view in person. The global network of natural history museums is an invaluable scientific resource. This work would not be possible without such places, both as repositories of specimens and highly talented people.

**Funding** Advanced European Research Council grant HADES-ERC “Benthic diagenesis and microbiology of hadal trenches” grant (agreement number 669947) awarded to Ronnie N Glud (University of Southern Denmark). Ship time provided by BMBF, Germany.

## Declarations

**Conflict of interest** The authors declare no competing interests.

**Ethics approval** All applicable international, national, and/or institutional guidelines for the care and use of animals were followed.

**Sampling and field studies** All necessary permits for sampling in Chile’s Exclusive Economic Zone were obtained by the authors from the Servicio Hidrográfico y Oceanográfico de la Armada de Chile. The study is compliant with CBD and Nagoya protocols.

**Data availability** Genetic sequences from the present study are available on GenBank (MN423252 for 16S, MN422493 for COI, and MN422494 for Cyt-b). Micro-CT data is available for download through MorphoSource: <https://www.morphosource.org/concern/media/000417515>.

**Author Contribution** Conceptualization: T.D.L., M.E.G., A.J.J.; Investigation: T.D.L., M.E.G., M.S.M., V.F., H.R., J.N.J.W., J.L.C.; Project administration: F.W., R.N.G.; Funding acquisition: F.W., R.N.G., A.J.J.; Resources: A.S.T., H.R., A.J.J.; Data curation: A.S.M., V.F., J.N.J.W., J.L.C.; Visualization: T.D.L., M.E.G., A.S.M., J.N.J.W.; Writing — original draft: T.D.L., M.E.G., H.R.; Writing — review and editing: all.

**Open Access** This article is licensed under a Creative Commons Attribution 4.0 International License, which permits use, sharing, adaptation, distribution and reproduction in any medium or format, as long as you give appropriate credit to the original author(s) and the source, provide a link to the Creative Commons licence, and indicate if changes were made. The images or other third party material in this article are included in the article’s Creative Commons licence, unless indicated otherwise in a credit line to the material. If material is not included in the article’s Creative Commons licence and your intended use is not permitted by statutory regulation or exceeds the permitted use, you will need to obtain permission directly from the copyright holder. To view a copy of this licence, visit <http://creativecommons.org/licenses/by/4.0/>.

## References

- Altschul SF, Gish W, Miller W, Myers EW, Lipman DJ (1990) Basic local alignment search tool. *J Mol Biol* 215:403–410
- Andriashev AP (1955) A new fish of the snailfish family (Pisces, Liparidae) found at a depth of more than 7 kilometers. *Trudy Inst Okeanol Akad Nauk SSSR* 12:340–344
- Andriashev AP (1975) A new ultra-abysal fish, *Notoliparis kurchatovi* gen. et sp. n. (Liparidae) from the South Orkney Trench (Antarctica). *Trudy Instituta Okeanologiya Akademia Nauk SSSR* 103:313–319
- Andriashev AP (1982) A review of fishes of the genus *Paraliparis* Collett (Liparidae) from the Kerguelen area, subantarctic. *Zoologicheskii zhurnal* 61:716–725
- Andriashev AP (1986) Review of the snailfish genus *Paraliparis* (Scorpaeniformes: Liparidae) of the Southern Ocean. *Koeltz, Koenigstein*
- Andriashev AP (1998) A review of recent studies of Southern Ocean Liparidae (Teleostei : Scorpaeniformes). *Cybiurn (Paris)* 22:255–266
- Andriashev AP (2003) Liparid fishes (Liparidae, Scorpaeniformes) of the Southern Ocean and adjacent waters. *Russian Academy of Sciences, Zoological Institute, Sankt-Petersburg*
- Andriashev AP, Stein DL (1998) Review of the snailfish genus *Careproctus* (Liparidae, Scorpaeniformes) in antarctic and adjacent waters. *Contrib Sci* 470:1–65
- Bell J (2008) A simple way to treat PCR products prior to sequencing using ExoSAP-IT. *Biotechniques* 44:834. <https://doi.org/10.2144/000112890>
- Bonaparte CL (1831) Saggio di una distribuzione metodica degli animali vertebrati. *Giornale Arcadico di Scienze Lettere ed Arti* 52:155–189
- Burke CV (1912) A new genus and six new species of fishes of the family Cyclogasteridae. *Proc U S Natl Mus* 43:567–574
- Butler RJ, Fernandez V, Nesbitt SJ, Leite JV, Gower DJ (2022) A new pseudosuchian archosaur, *Mambawakale ruhuhu* gen. et sp. nov., from the Middle Triassic Manda Beds of Tanzania. *R Soc Open Sci* 9:211622. <https://doi.org/10.1098/rsos.211622>
- Byrkjedal I, Rees DJ, Willassen E (2007) Lumping lumpsuckers: molecular and morphological insights into the taxonomic status of *Eumicrotremus spinosus* (Fabricius, 1776) and *Eumicrotremus eggvini* Koefoed, 1956 (Teleostei: Cyclopteridae). *J Fish Biol* 71: 111–131. <https://doi.org/10.1111/j.1095-8649.2007.01550.x>
- Chernova NV (2008) Systematics and phylogeny of fish of the genus *Liparis* (Liparidae, Scorpaeniformes). *J Ichthyol* 48:831–852. <https://doi.org/10.1134/S0032945208100020>
- Chernova NV, Prut’ko VG (2011) Two new species of *Paraliparis* (Scorpaeniformes: Liparidae) from the Ross Sea (Antarctica). *J Ichthyol* 51:363–372. <https://doi.org/10.1134/S0032945211030015>
- Chernova NV, Stein DL, Andriashev AP (2004) family Liparidae Scopoli 1777 - snailfishes. *Annotated Check lists of Fishes* 31:72
- Cohen DM (1968) The cyclopterid genus *Paraliparis*, a senior synonym of *Gymnolycodes* and *Eutelichthys*, with the description of a new species from the Gulf of Mexico. *Copeia* 1968:384–388
- Collett R (1879) Fiske fra Nordhavs-Expeditionens sidste Togt, Sommeren 1878. *Forh Vidensk Selsk Christiania (for 1878)* 14:1–106
- Darriba D, Taboada GL, Doallo R, Posada D (2012) jModelTest 2: more models, new heuristics and parallel computing. *Nat Methods* 9:772. <https://doi.org/10.1038/nmeth.2109>
- Dettaï A, Lautredou AC, Bonillo C, Goimbault E, Busson F, Causse R, Couloux A, Cruaud C, Duhamel G, Denys G, Hauteceour M, Iglesias S, Koubbi P, Lecointre G, Moteki M, Pruvost P, Tercier S, Ozouf C (2011) The actinopterygian diversity of the CEAMARC cruises: barcoding and molecular taxonomy as a multi-level tool for new findings. *Deep-Sea Res II Top Stud Oceanogr* 58:250–263. <https://doi.org/10.1016/j.dsr2.2010.05.021>

- Dingerkus G, Uhler LD (1977) Enzyme clearing of alcian blue stained whole small vertebrates for demonstration of cartilage. *Stain Technol* 52:229–232. <https://doi.org/10.3109/10520297709116780>
- Drummond AJ, Ho SY, Phillips MJ, Rambaut A (2006) Relaxed phylogenetics and dating with confidence. *PLoS Biol* 4:e88. <https://doi.org/10.1371/journal.pbio.0040088>
- Duhamel G, Hauteceur M, Dettai A, Causse R, Pruvost P, Busson F, Couloux A, Koubbi P, Williams R, Ozouf-Costaz C, Nowara G (2010) Liparids from the Eastern sector of Southern Ocean and first information from molecular studies. *Cybius* 34:319–343
- Fricke R, Eschmeyer WN, Van der Laan R (eds) (2020) Eschmeyer's catalog of fishes: genera, species, references. <http://researcharchive.calacademy.org/research/ichthyology/catalog/fishcatmain.asp>. Electronic version accessed 15 Mar 2020
- Froese R, Pauly D (eds) (2021) FishBase. [www.fishbase.org](http://www.fishbase.org). Electronic version accessed 22 Jun 2021
- Fujii T, Jamieson AJ, Solan M, Bagley PM, Priede IG (2010) A large aggregation of liparids at 7703 meters and a reappraisal of the abundance and diversity of hadal fish. *BioScience* 60:506–515. <https://doi.org/10.1525/bio.2010.60.7.6>
- Garman S (1892) The discoboli. cyclopteridae, liparopsidae, and liparididae. *Memoirs of the Museum of Comparative Zoology* 14(pt 2):1–96, Pls. 1–13
- Garman S (1899) Reports on an exploration off the west coast of Mexico, Central and South America, and off the Galapagos Islands, in charge of Alexander Agassiz, by the US Fish Commission steamer "Albatross" during 1891, Lieut. Commanding. XXVI. *Memoirs of the Museum of Comparative Zoology at Harvard College* 24:431
- GEBCO (2015) General bathymetric chart of the oceans. GEBCO\_2014 Grid. [http://www.gebco.net/data\\_and\\_products/gridded\\_bathymetry\\_data/gebco\\_30\\_second\\_grid](http://www.gebco.net/data_and_products/gridded_bathymetry_data/gebco_30_second_grid). Electronic version accessed 7 May 2015
- Gerringer ME (2019) On the success of the hadal snailfishes. *Integr Org Biol* 1:1–18. <https://doi.org/10.1093/iob/obz004>
- Gerringer ME, Drazen JC, Linley TD, Summers AP, Jamieson AJ, Yancey PH (2017a) Distribution, composition and functions of gelatinous tissues in deep-sea fishes. *R Soc Open Sci* 4:171063. <https://doi.org/10.1098/rsos.171063>
- Gerringer ME, Linley TD, Jamieson AJ, Goetze E, Drazen JC (2017b) *Pseudoliparis swirei* sp. nov.: a newly-discovered hadal snailfish (Scorpaeniformes: Liparidae) from the Mariana Trench. *Zootaxa* 4358:161–177. <https://doi.org/10.11646/zootaxa.4358.1.7>
- Gerringer ME, Linley TD, Nielsen JG (2021) Revision of the depth record of bony fishes with notes on hadal snailfishes (Liparidae, Scorpaeniformes) and cusk eels (Ophidiidae, Ophidiiformes). *Mar Biol* 168. <https://doi.org/10.1007/s00227-021-03950-8>
- Gerringer ME, Popp BN, Linley TD, Jamieson AJ, Drazen JC (2017c) Comparative feeding ecology of abyssal and hadal fishes through stomach content and amino acid isotope analysis. *Deep Sea Res Part I Oceanogr Res Pap* 121:110–120. <https://doi.org/10.1016/j.dsr.2017.01.003>
- Gill TN (1861) Catalogue of the fishes of the eastern coast of North America, from Greenland to Georgia. *Proc Acad Natl Sci Phila* 13:1–61
- Guindon S, Dufayard JF, Lefort V, Anisimova M, Hordijk W, Gascuel O (2010) New algorithms and methods to estimate maximum-likelihood phylogenies: assessing the performance of PhyML 3.0. *Syst Biol* 59:307–321. <https://doi.org/10.1093/sysbio/syq010>
- Günther A (1887) REPORT on the deep-sea fishes collected by H.M.S. Challenger during the Years 1873–76
- Hasegawa M, Kishino H, Yano T (1985) Dating of the human-ape splitting by a molecular clock of mitochondrial DNA. *J Mol Evol* 22:160–174. <https://doi.org/10.1007/BF02101694>
- HeliconSoft (2017) Helicon remote and helicon focus. HeliconSoft, Ukraine, pp Image stacking software
- Horton T, Marsh L, Bett BJ, Gates AR, Jones DOB, Benoist NMA, Pfeifer S, Simon-Lledó E, Durden JM, Vandepitte L, Appeltans W (2021) Recommendations for the standardisation of open taxonomic nomenclature for image-based identifications. *Front Mar Sci*:8. <https://doi.org/10.3389/fmars.2021.620702>
- Imamura H, Abe MY (2002) Demise of the Scorpaeniformes (Actinopterygii: Percomorpha): an alternative phylogenetic hypothesis. *Bull Fish Sci Hokkaido Univ* 53:107–128
- Jamieson AJ (2015) The hadal zone. Cambridge University Press, Cambridge
- Jamieson AJ, Fujii T, Mayor DJ, Solan M, Priede IG (2010) Hadal trenches: the ecology of the deepest places on Earth. *Trends Ecol Evol* 25:190–197
- Jamieson AJ, Linley TD, Eigler S, Macdonald T (2021) A global assessment of fishes at lower abyssal and upper hadal depths (5000 to 8000 m). *Deep-Sea Res I Oceanogr Res Pap* 178:103642. <https://doi.org/10.1016/j.dsr.2021.103642>
- Kai Y, Murasaki K, Misawa R, Fukui A, Morikawa E, Narimatsu Y (2020) A new species of snailfish of the genus *Paraliparis* (Liparidae) from the western North Pacific, with a redescription of the poorly known species *Paraliparis mandibularis*. *Zookeys* 968:143–159. <https://doi.org/10.3897/zookeys.968.56057>
- Kenchington EL, Baillie SM, Kenchington TJ, Bentzen P (2017) Barcoding Atlantic Canada's mesopelagic and upper bathypelagic marine fishes. *PLoS One* 12:e0185173. <https://doi.org/10.1371/journal.pone.0185173>
- Kido K (1988) Phylogeny of the family Liparididae, with the taxonomy of the species found around Japan. *Mem Fac Fish Hokkaido Univ* 35:125–256
- Kim DW, Yoo WG, Park HC, Yoo HS, Kang DW, Jin SD, Min HK, Paek WK, Lim J (2012) DNA barcoding of fish, insects, and shellfish in Korea. *Genomics Inform* 10:206–211. <https://doi.org/10.5808/GI.2012.10.3.206>
- Kimura M (1981) Estimation of evolutionary distances between homologous nucleotide sequences. *Proc Natl Acad Sci U S A* 78:454–458. <https://doi.org/10.1073/pnas.78.1.454>
- Kneibelsberger T, Landi M, Neumann H, Kloppmann M, Sell AF, Campbell PD, Laakmann S, Raupach MJ, Carvalho GR, Costa FO (2014) A reliable DNA barcode reference library for the identification of the North European shelf fish fauna. *Mol Ecol Resour* 14:1060–1071. <https://doi.org/10.1111/1755-0998.12238>
- Knudsen SW, Møller PR, Gravlund P (2007) Phylogeny of the snailfishes (Teleostei: Liparidae) based on molecular and morphological data. *Mol Phylogenet Evol* 44:649–666. <https://doi.org/10.1016/j.ympev.2007.04.005>
- Krøyer HN (1862) Nogle Bidrag til Nordisk ichthyologi [with subsections under separate titles]. *Naturhist Tidsskr Kjøbenhavn* 1:233–310
- Kumar S, Stecher G, Li M, Knyaz C, Tamura K (2018) MEGA X: molecular evolutionary genetics analysis across computing platforms. *Mol Biol Evol* 35:1547–1549. <https://doi.org/10.1093/molbev/msy096>
- Linley TD, Gerringer ME, Yancey PH, Drazen JC, Weinstock CL, Jamieson AJ (2016) Fishes of the hadal zone including new species, *in situ* observations and depth records of Liparidae. *Deep Sea Res Part I Oceanogr Res Pap* 114:99–110. <https://doi.org/10.1016/j.dsr.2016.05.003>
- Linley TD, Stewart AL, McMillan PJ, Clark MR, Gerringer ME, Drazen JC, Fujii T, Jamieson AJ (2017) Bait attending fishes of the abyssal zone and hadal boundary: community structure, functional groups and species distribution in the Kermadec, New Hebrides and Mariana trenches. *Deep Sea Res Part I Oceanogr Res Pap* 121:38–53. <https://doi.org/10.1016/j.dsr.2016.12.009>
- Löytynoja A, Goldman N (2010) webPRANK: a phylogeny-aware multiple sequence aligner with interactive alignment browser. *BMC Bioinform* 11:579. <https://doi.org/10.1186/1471-2105-11-579>

- Mabragaña E, Delpiani SM, Rosso JJ, González-Castro M, Deli Antoni M, Hanner R, Díaz de Astarloa JM (2016) Barcoding Antarctic fishes: species discrimination and contribution to elucidate ontogenetic changes in Nototheniidae. In: Trivedi S, Ansari AA, Ghosh SK, Rehman H (eds) DNA barcoding in marine perspectives. Springer International Publishing, Cham, pp 213–242
- Matallanas J, Pequeño G (2000) A new snailfish species, *Paraliparis orcadensis* sp. nov. (Pisces: Scorpaeniformes) from the Scotia Sea (Southern Ocean). Polar Biol 23:298–300. <https://doi.org/10.1007/s003000050448>
- McCusker MR, Denti D, Van Guelpen L, Kenchington E, Bentzen P (2013) Barcoding Atlantic Canada's commonly encountered marine fishes. Mol Ecol Resour 13:177–188. <https://doi.org/10.1111/1755-0998.12043>
- Mecklenburg CW, Möller PR, Steinke D (2011) Biodiversity of arctic marine fishes: taxonomy and zoogeography. Mar Biodivers 41:109–140. <https://doi.org/10.1007/s12526-010-0070-z>
- Miya M, Takeshima H, Endo H, Ishiguro NB, Inoue JG, Mukai T, Satoh TP, Yamaguchi M, Kawaguchi A, Mabuchi K, Shirai SM (2003) Major patterns of higher teleostean phylogenies: a new perspective based on 100 complete mitochondrial DNA sequences. Mol Phylogenet Evol 26:121–138
- Nielsen JG (1964) Fishes from depths exceeding 6000 meters. Galathea Report 7:113–124
- Orlov AM, Tokranov AM (2011) Some rare and insufficiently studied snailfish (Liparidae, Scorpaeniformes, Pisces) in the Pacific waters off the Northern Kuril Islands and Southeastern Kamchatka, Russia. ISRN Zoology 2011:1–12. <https://doi.org/10.5402/2011/341640>
- Orr JW, Pitruk DL, Manning R, Stevenson DE, Gardner JR, Spies I (2020) A new species of snailfish (Cottiformes: Liparidae) closely related to *Careproctus melanurus* of the Eastern North Pacific. Copeia 108. <https://doi.org/10.1643/ci2020008>
- Orr JW, Spies I, Stevenson DE, Longo GC, Kai Y, Ghods SAM, Hollowed M (2019) Molecular phylogenetics of snailfishes (Cottoidei: Liparidae) based on MtDNA and RADseq genomic analyses, with comments on selected morphological characters. Zootaxa 4642:1–79. <https://doi.org/10.11646/zootaxa.4642.1.1>
- Pallas PS (1769) Spicilegium Zoologica quibus novae imprimis et obscurae animalium species iconibus, descriptionibus atque commentariis illustrantur. Berolini, Gottl 1:1–42
- Priede IG, Froese R (2013) Colonization of the deep sea by fishes. J Fish Biol 83:1528–1550. <https://doi.org/10.1111/jfb.12265>
- Rambaut A (2012) FigTree v1.4.3. Institute of Evolutionary Biology, University of Edinburgh, Edinburgh. <http://tree.bio.ed.ac.uk/software/figtree/>
- Robertson DR, Angulo A, Baldwin CC, Pitassy D, Driskell A, Weigt L, Navarro IJF (2017) Deep-water bony fishes collected by the B/O Miguel Oliver on the shelf edge of Pacific Central America: an annotated, illustrated and DNA-barcoded checklist. Zootaxa 4348: 1–125. <https://doi.org/10.11646/zootaxa.4348.1.1>
- Rock J, Costa FO, Walker DI, North AW, Hutchinson WF, Carvalho GR (2008) DNA barcodes of fish of the Scotia Sea, Antarctica indicate priority groups for taxonomic and systematics focus. Antart Sci 20: 253–262. <https://doi.org/10.1017/s0954102008001120>
- Sabaj MH (2016) Standard symbolic codes for institutional resource collections in herpetology and ichthyology: an Online Reference. Version 6.5 (16 August 2016). Electronically accessible at <http://www.asih.org/>, American Society of Ichthyologists and Herpetologists, Washington, DC. Electronic version accessed 3 Nov 2016
- Sigovini M, Keppel E, Tagliapietra D, Isaac N (2016) Open nomenclature in the biodiversity era. Methods Ecol Evol 7:1217–1225. <https://doi.org/10.1111/2041-210x.12594>
- Smith PJ, Steinke D, Dettai A, McMillan P, Welsford D, Stewart A, Ward RD (2012) DNA barcodes and species identifications in Ross Sea and Southern Ocean fishes. Polar Biol 35:1297–1310. <https://doi.org/10.1007/s00300-012-1173-8>
- Solomatov SF, Orlov AM (2018) Smooth lumpsucker *Aptocyclus ventricosus* in the northwestern Sea of Japan: distribution and some life history traits. Arch Pol Fish 26:5–20. <https://doi.org/10.2478/aopf-2018-0002>
- Stein DL (1978) A Review of the deepwater Liparidae (Pisces) from the coast of Oregon and adjacent waters. Calif Acad Sci 127:55
- Stein DL (2005) Descriptions of four new species, redescription of *Paraliparis membranaceus*, and additional data on species of the fish family Liparidae (Pisces, Scorpaeniformes) from the west coast of South America and the Indian Ocean. Zootaxa 1019:1–25
- Stein DL (2012) Snailfishes (Family Liparidae) of the Ross Sea, Antarctica, and closely adjacent waters. Zootaxa 3285:1–120
- Stein DL (2016) Description of a new hadal *Notoliparis* from the Kermadec Trench, New Zealand, and redescription of *Notoliparis kermadecensis* (Nielsen) (Liparidae, Scorpaeniformes). Copeia 104: 907–920. <https://doi.org/10.1643/C1-16-451>
- Stein DL, Chernova NV (2002) First records of snailfishes (Pisces: Liparidae) from the Galapagos Islands, with descriptions of two new species, *Paraliparis darwini* and *Paraliparis galapagosensis*. Proc Calif Acad Sci 53:151–160
- Stein DL, Chernova NV, Andriashev AP (2001) Snailfishes (Pisces: Liparidae) of Australia, including descriptions of thirty new species. Rec Aust Mus 53:341–406
- Stein DL, Meléndez RC, Kong IU (1991) A review of Chilean snailfishes (Liparididae, Scorpaeniformes) with descriptions of a new genus and three new species. Copeia 1991:358–373
- Steinke D, Zemplak TS, Boutillier JA, Hebert PDN (2009) DNA barcoding of Pacific Canada's fishes. Mar Biol 156:2641–2647. <https://doi.org/10.1007/s00227-009-1284-0>
- Suchard MA, Lemey P, Baele G, Ayres DL, Drummond AJ, Rambaut A (2018) Bayesian phylogenetic and phylodynamic data integration using BEAST 1.10. Virus Evol 4:vey016. <https://doi.org/10.1093/ve/vey016>
- Tamura K, Nei M (1993) Estimation of the number of nucleotide substitutions in the control region of mitochondrial DNA in humans and chimpanzees. Mol Biol Evol 10:512–526. <https://doi.org/10.1093/oxfordjournals.molbev.a040023>
- Taylor WR (1967) An enzyme method of clearing and staining small vertebrates. Proc U S Natl Mus 122:1–17
- The Inkscape Team (2017) Inkscape v. 0.92.2. <https://inkscape.org/>. Accessed 17 Oct 2017
- Wiley EO, Johnson GD (2010) A teleost classification based on monophyletic groups. In: Nelson JS, Schultze H-P, Wilson MVH (eds) Origin and Phylogenetic Interrelationships of Teleosts. Verlag Dr. Friedrich Pfeil, München, pp 123–182
- Zhang J-B, Hanner R (2011) DNA barcoding is a useful tool for the identification of marine fishes from Japan. Biochem Syst Ecol 39: 31–42. <https://doi.org/10.1016/j.bse.2010.12.017>

**Publisher's note** Springer Nature remains neutral with regard to jurisdictional claims in published maps and institutional affiliations.